Computed tomography features of acinar cell carcinoma of the pancreas

M. Barat, A. Dohan, S. Gaujoux, C. Hoeffel, D. Jornet, A. Oudjit, R. Coriat, M. Barret, B. Terris, P. Soyer

Abstract

Purpose: To report the computed tomography (CT) features of pancreatic acinar cell carcinoma (ACC) and identify CT features that may help discriminate between pancreatic ACC and pancreatic ductal adenocarcinoma (PDA).

Materials and methods: The CT examinations of 20 patients (13 men, 7 women; mean age, 66.5 ± 10.7 [SD] years (range: 51 - 88 years) with 20 histopathologically proven pancreatic ACC were reviewed. CT images were analyzed qualitatively and quantitatively and compared to those obtained in 20 patients with PDA. Comparisons were performed using univariate analysis with a conditional logistic regression model.

Results: Pancreatic ACC presented as an enhancing (20/20; 100%), oval (15/20; 75%), well-delineated (14/20; 70%), and purely solid (13/20; 65%) pancreatic mass with a mean diameter of 52.6 ± 28.0 (SD) mm (range: 24 – 120 mm) in association with visible lymph nodes (14/20; 70%). At univariate analysis, well-defined margins (Odds ratio [OR], 7.00; P = 0.005), nondilated bile ducts (OR, 9.00; P = 0.007), visible lymph nodes (OR, 4.33; P = 0.028) and adjacent organ involvement (OR, 5.67; P = 0.02) were the most discriminating CT features to differentiate pancreatic ACC from PDA. When present, lymph nodes were larger in patients with pancreatic ACC (14 ± 4.8 [SD]; range: 7 - 25 mm) than in those with PDA (8.8 ± 4.1 [SD]; range: 5 - 15 mm) (P = 0.039).

Conclusion: On CT, pancreatic ACC presents as an enhancing, predominantly oval and purely solid pancreatic mass that most frequently present with no bile duct dilatation, no visible lymph nodes, no adjacent organ involvement and larger visible lymph nodes compared to PDA.

Keywords: Tomography, X-ray computed; Carcinoma, acinar cell; Pancreatic neoplasms

Highlights

- ✓ *Absence of bile duct dilatation is the most discriminating variable for the diagnosis of pancreatic acinar cell carcinoma.*
- ✓ *Hepatic metastases, visible lymph nodes and involvement of adjacent organ are discriminating and independently associated variables for the diagnosis of pancreatic acinar cell carcinoma.*
- ✓ *CT helps diagnose pancreatic acinar cell carcinoma in the presence of several categorical findings, which are more frequently observed in pancreatic acinar cell carcinoma than in pancreatic ductal adenocarcinoma.*

Abbreviations

ACC: Acinar cell carcinoma

CI: Confidence interval

CT: Computed tomography

MRI: Magnetic resonance imaging

OR: Odds ratio

PDA: Pancreatic ductal adenocarcinoma

SD: Standard deviation

Introduction

Pancreatic ductal adenocarcinoma (PDA) accounts for the majority of solid pancreatic tumors [1]. However, the pancreas can be involved by many other tumors so that one role of imaging is lesion characterization [2-4]. Although magnetic resonance imaging, owing to higher degrees of tissue characterization, can provide useful information, computed tomography (CT) is still considered as the first line and standard imaging for the diagnosis of pancreatic tumors [5, 6].

Pancreatic acinar cell carcinoma (ACC) is a rare tumor that represents less than 1% of all pancreatic neoplasms and arises from acinar elements of the exocrine pancreas [7,8]. The specific diagnosis of ACC of the pancreas is often delayed because patients with this condition may present with nonspecific symptoms similar to those observed in patients with the more common PDA [8]. Moreover, a definite histopathological diagnosis may be difficult using the small samples obtained with fine-needle biopsy [9,10]. Another difficulty is that specific histochemical stains, which are required to ascertain the diagnosis, are not performed routinely [10]. As a result, imaging should have a major importance to alert the clinician and the pathologist, should imaging findings be consistent with the diagnosis of pancreatic ACC. This role is rendered more critical because it is commonly admitted that ACC conveys a better prognosis than PDA and that patients with pancreatic ACC may benefit of a more aggressive surgical approach [7,8,11].

The CT features of pancreatic ACC have been described in several studies and some suggestive features have been identified [10,12-18]. However, ACC of the pancreas may sometimes display nonspecific or misleading features on CT [9,14,19,20,21]. In addition, the capabilities of CT in discriminating between pancreatic ACC and PDA have not been elucidated yet because in the single study that made such comparison, only six patients with

pancreatic ACC were included and the comparison was restricted to tumor enhancement patterns [22].

The purpose of this study was to report the CT presentation of pancreatic ACC and identify findings that might help discriminate between pancreatic ACC and PDA.

Methods

Patients

The databases of the departments of pathology, surgery and gastroenterology of our institutions were queried from January 2007 to December 2018. The initial search retrieved 29 patients with possibly pancreatic ACC. Two patients were excluded because they ultimately had other tumor than ACC. A cross-match was performed with the radiology departments' database to identify those who had undergone CT examination in our institutions. Seven patients were further excluded because they had CT examinations performed at another institution and not available for review (n = 2) or because the initial CT examination before neoadjuvant chemotherapy was not available (n = 5). Figure 1 summarizes patients inclusion.

The study population consisted of 20 patients (13 men, 7 women) with pancreatic ACC with a mean age of 66.5 ± 10.7 (standard deviation [SD]) years (range: 51-88 years) (Table 1). The diagnosis of ACC was obtained after histopathological analysis of biopsy specimens obtained before any treatment. According to the 8th edition of the American Joint Commission on Cancer (AJCC) TNM staging system [23], 6/20 patients (30%) had T2 ACC, 8/20 patients (40%) had T3 ACC, and 6/20 patients (30%) had T4 ACC.

Twenty patients with PDA were identified for matched comparison. They were extracted from a database of 350 patients with histopathologically confirmed PDA. These 20 patients were thus selected according to gender, age, tumor T stage, treatment and had CT examination during the same period with the same CT protocols than those with ACC. There were 13 men and 7 women, with a mean age of 61.8 ± 7.5 (SD) years (range: 43-74 years). For the 20 patients, the diagnosis of PDA was obtained after histopathological analysis of biopsy specimens obtained before any treatment. In this group, 5/20 patients (25%) had T2 PDA, 6/20 patients (30%) had T3 PDA, and 9/20 patients (45%) had T4 PDA.

This retrospective multicenter study received local ethics and institutional review board committee approval. According to the retrospective design, the institutional review boards waived the requirement for written informed consent.

CT protocol

CT examinations were performed with different CT units including Somatom Sensation® 64 (Siemens Healthineers), Somatom Definition® Flash (Siemens Healthineers) and Revolution HD® (General-Electric Healthcare). The following CT parameters were used: field-of-view, 279 – 450 mm; beam collimation, 38.4 - 40 mm (64×0.6-0.625 mm collimator setting); slice thickness, 1 - 1.25 mm; peak tube potential, 110-120 kVp; gantry revolution time, 0.5 s; and beam pitch, 0.984 - 1.2.

A total of 100 - 120 mL of contrast material (iomeprol, Iomeron 350®, Bracco Imaging, or iobitridol, Xenetix 350®, Guerbet) was injected intravenously using an automated power injector at a rate of 2.5-4 mL/s. An unenhanced imaging set was first obtained. A second imaging set was obtained during the arterial phase (30 s after initiating contrast material administration) using an automatic triggering acquisition. A third set was obtained during the portal phase with a mean delay of 70 s.

CT Image analysis

For this retrospective study, two radiologists reviewed the CT examinations on a picture archiving and communication system viewing station (Directview, 12.1.0365 version, Carestream Health Inc.) using a standardized form in a joint session. Anonymized CT examinations were analyzed for tumor presentation, including quantitative and qualitative variables. Axial images were interpreted along with multiplanar, three-dimensional and maximum intensity projection images. To minimize review bias, the radiologists were blinded to any patient information. In addition, they did not participate to the CT examinations at the time they were performed. Agreement was reached by consensus.

Several findings were evaluated by using a standardized data collection form (Table 2). The following features of ACC were evaluated including largest transverse diameter of the tumor, tumor location (head, body or tail), tumor shape (oval or round), margin (well or ill-defined contours) and presence of a tumor capsule. CT examinations were also analyzed for tumor content (purely solid, cystic or mixed), presence or internal necrosis/hemorrhage, homogeneity of tumor enhancement after intravenous administration of iodinated contrast material, degree of tumor enhancement relative to the apparently uninvolved pancreas on arterial and portal phases, internal calcification, presence of main pancreatic duct dilatation (diameter > 4 mm), upstream pancreatic atrophy, vascular involvement by tumor, segmental portal hypertension, hepatic metastases, bile duct dilatation, presence of visible lymph nodes,

largest axial diameter of visible lymph nodes, direct involvement of adjacent organ, and ascites.

Non enhancing areas with attenuation similar to that of the gallbladder on unenhanced CT images were considered as necrotic/hemorrhagic components of the tumor, whereas the others were considered solid. Tumor enhancement was considered present when enhancement was identified on CT images obtained after intravenous administration of iodinated contrast material, whatever the specific imaging phase. Calcifications were searched on unenhanced images. Vascular involvement was considered for involvement of any vascular structure (arterial or venous) identified on CT images.

Statistical analysis

Statistical analysis was performed using software (SAS, V 9.3, SAS Institute; R-3, R Project). Descriptive statistics were calculated for all variables evaluated at CT. Quantitative data were reported as means, SD, medians, first quartiles, third quartiles and ranges. Qualitative data were reported as raw numbers, proportions, and percentages. Comparison of qualitative variables was made with Fisher exact test using Freeman-Halton extension when needed [24]. Comparisons of quantitative variables were performed with Mann-Whitney U test. Sensitivity, specificity and accuracy of each variable for the diagnosis of ACC were calculated with their corresponding 95% confidence interval (CI). Quantitative variables were then entered into univariate analysis with a conditional logistic regression model to identify factors associated with ACC at CT. Significance was set at $P < 0.05$.

Results

Results of descriptive statistics

No differences in age and sex distribution were found between patients with ACC and those with PDA (Table 1). The results of descriptive analysis are reported in Table 3. Sensitivity, specificity, and accuracy of qualitative variables are reported in Table 4 with corresponding 95% CIs.

ACC presented as enhancing (20/20; 100%), oval (15/20; 75%), purely solid (13/20; 65%) pancreatic mass with well-defined margins (14/20; 70%), with a mean diameter of 52.6 ± 28.0 (SD) mm (range: 24–120 mm) in association with visible lymph nodes (14/20; 70%) (Fig. 2). Visible lymph nodes were more frequent in ACCs compared to PDAs ($P = 0.039$)

whereas no differences in visible lymph node largest diameter were found. ACCs were less frequently hypoattenuating relative to the apparently uninvolved pancreatic parenchyma on the arterial phase than PDAs ([9/20; 45%] *vs.* [17/20; 85%], respectively) (P = 0.009) and more frequently presented with well-defined tumor margins than PDAs (P = 0.005).

Well-defined tumor margins were more frequently observed in ACCs (14/20; 70%) compared to PDAs (5/20; 25%) (P = 0.005) and this finding was the most accurate one (73 % accuracy) for the diagnosis of ACC. Absence of bile duct dilatation was more frequently observed in ACCs (2/20; 10%) compared to PDAs (10/20; 50%) (P = 0.014) and had 70% accuracy for the diagnosis of ACC. Involvement of adjacent organs by pancreatic tumor was more frequently observed in ACCs (10/20; 50%) compared to PDAs (3/20; 15%) (P = 0.041) (Figs. 3, 4) and this finding had 85 % specificity (17/20; 95% CI: 62 - 97%) for the diagnosis of ACC. The involved organs by ACC were the duodenum (4 patients), the stomach (3 patients), the spleen (2 patients) and the left adrenal gland (1 patient). No significant differences were found between patients with ACC and those with PDA for all other quantitative variables (Table 3). Tumor encapsulation and internal calcification had 100 % specificity for the diagnosis of ACC but these findings were visible in only 3/20 (15%) and 2/20 ACCs (10%), respectively (Figs. 3, 4). In the six patients with ACC and main pancreatic duct dilatation, the dilatation was due to external compression by ACC in four patients and direct extent of tumor into the main pancreatic duct in two patients.

Results of univariate analysis

The results of univariate analysis are reported in **Table 5**. The absence of bile duct dilatation was the most discriminating feature for the diagnosis of pancreatic ACC (P = 0.007). The presence of visible lymph nodes (P = 0.028) and involvement of adjacent organ (P = 0.020) were the other most discriminating features for the diagnosis of pancreatic ACC.

Discussion

In the present study we have reported the CT features of pancreatic ACC in 20 patients. The diagnosis of pancreatic ACC may be suggested by the presence of several categoric CT findings, which are more frequently observed in patients with ACC than in those with PDA. Of these, well-defined margins and absence of bile duct dilatation are the two most discriminating CT features for the diagnosis of ACC. However, presence of visible lymph nodes and involvement of adjacent organ are also significantly associated with ACC.

Differentiation between ACC and PDA is difficult because patients may present with similar symptoms [7,8]. It can be assumed that knowledge of discriminating findings may help clinicians and pathologists consider the diagnosis of ACC in patients with pancreatic tumors.

In our study, well-defined tumor margins was the most discriminating variable to differentiate ACC from PDA and yielded the highest accuracy for the diagnosis of ACC. This finding had a prevalence of 33%-91% in other studies [18,25,26]. On the opposite, PDA more often presents with ill-defined margins [25]. In our study, the absence of bile duct dilatation was another discriminating variable to differentiate ACC from PDA. Only 2/20 patients (10%) with ACC had bile duct dilatation compared to 10/20 patients (50%) with PDA. Our results are consistent with those of other researchers who reported bile duct dilatation in only 7%-17% of patients with pancreatic ACC [8,10,16]. The low prevalence of bile duct dilatation in ACC may be due to the fact that it does not originate from the ductal epithelium [20] and bile duct dilatation might be due to intrahepatic bile duct metastases of ACC [27]. Of interest, in our study, the location of pancreatic tumors cannot be considered as a confounding factor since 9/20 tumors were located in the pancreatic head in both groups.

The presence of visible lymph nodes on CT was another discriminating feature to differentiate pancreatic ACC from PDA. In our study, visible lymph nodes were present in 14/20 patients (70%) with ACC. This figure is greater than those reported by other researchers [14,15,16,18]. Raman et al. reported significant peripancreatic lymphadenopathy (*i.e.,*>10 mm in short axis) in 5/15 patients (30%) with pancreatic ACC [16]; of note, 9/15 patients (60%) had at least one malignant peripancreatic lymph node identified at surgery, indicating that CT underperforms in the detection of metastatic lymph nodes [16]. Other studies reported visible lymphadenopathy on CT in 3/10 (30%) [18], 4/10 (40%) [15] and 3/5 patients (60%) [14] with pancreatic ACC.

In our study, hypoattenuating tumor on the arterial phase was more frequently observed in PDA. In general, ACC are hypoattenuating relative to the pancreas [22,25] and poorly vascularized tumors [28]. One study described all pancreatic ACCs as hypoattenuating at large but no specific analysis of attenuation was made for individual CT phases [25]. However, ACC can also be hyperattenuating during the arterial phase on CT [17] and hyperenhancing after intravenous administration of mangafodipir trisodium on MRI [29]. In another study all PDAs were hypoattenuating on all imaging phases (unenhanced, arterial, portal and delayed phases) on CT, with a peak enhancement during the portal phase in 4/6 or the arterial phase in 2/6 pancreatic ACC [22].

We observed involvement of adjacent organ by pancreatic ACC in 10/20 patients (50%). This finding was a discriminating variable for the diagnosis of ACC. Data from the literature confirm that adjacent organ involvement by ACC is not rare [14, 15, 25, 30]. Chiou et al. observed local invasion of adjacent organs in 4/10 patients (40%) with pancreatic ACC on CT [15]. In the study by Tatli et al., 4/11 pancreatic ACC (36%) invaded the adjacent duodenum [25]. Gravante et al. reported one patient with ACC of the pancreas that invaded the gastric wall [30]. In Liu et al. study, 3/5 patients (60%) with pancreatic ACC presented with involvement of adjacent organs, consisting in duodenal, splenic, and renal involvement [14]. Khalili et al. reported one ACC of the pancreatic tail that involved the small bowel [31].

Tumor encapsulation was observed in three ACCs in our study. Although this finding was 100% specific for the diagnosis of ACC, it was observed in only 3 ACCs. However, encapsulation has been reported in other tumors [9,32]. As a consequence, tumor capsule may be a misleading finding and ACC may occasionally resemble solid and papillary tumor of the pancreas [9]. The prevalence of encapsulation in ACC varies among studies. In the study by Liu et al. none of the five ACCs displayed encapsulation [14] whereas Hu et al. [18], Hsu et al. [26], Chiou et al. [15] and Raman et al. [16] reported encapsulation in 7/10 (70 %), 4/6 (67 %), 6/10 (60 %) and 8/15 pancreatic ACCs (53 %), respectively. The variation in prevalence may be due to variation in interpretation. In this regard, ACC initially develops into the pancreas and histopathological studies showed that the capsule corresponds to compressed pancreatic parenchyma around the tumor [31].

Several authors have described internal calcifications in pancreatic ACC, with a prevalence ranging from 7% (2/30 ACC) [10] to 50% (5/10 ACC) [15]. Of note, in the study by Raman et al. none of 15 pancreatic ACC contained calcifications on CT [16]. This finding was present in only 2/20 ACC (10 %) in our study and absent in all PDAs. However, some reports have described the presence of internal calcifications in PDAs [33]. However, it is commonly admitted that calcifications in PDA mostly occurs in patients with preexisting chronic calcific pancreatitis and predominantly within the nonneoplastic pancreatic tissue [34]. From a more general point of view, internal calcifications are observed in myriad pancreatic lesions [33].

In the present study, pancreatic ACCs were homogeneously distributed between the head, boy and tail consistent with other studies [10,14,16,18]. Regarding tumor size, we did not find significant differences in largest tumor diameter between ACCs and PDAs. However, it is commonly admitted that pancreatic ACC usually presents as a large tumor with a mean diameter of up to 7.1 cm [18] and largest diameter of up to 12 cm [28]. However, a wide

range has been reported with mean diameters of 3.2 cm [9], 5.1cm [16], 5.3 cm [8,14], 6 cm [25], 6.1 cm [26] and 7 cm [10]. By comparison, PDA usually presents with a mean diameter of 2-3 cm [35]. In one surgical study comparing lesion diameter, a significant difference was found between pancreatic ACC (median, 54 mm) and PDA (median, 31 mm) ($P < 0.001$) at histopathological analysis [11].

Researchers have reported unusual imaging features of pancreatic ACC [9,21]. Luo et al. have reported two ACCs presenting as diffuse enlargement of the pancreatic gland displaying a "sausage-like" shape [21]. Hashimito et al. have reported similar feature in one patient [20]. In our study, no patients had pancreatic ACC featuring a "sausage-like" shape.

In our patients with main pancreatic duct dilatation two patterns were observed; one consisted in enlarged pancreatic duct abutting to tumor and the other in an intraluminal extent of ACC. When present, this latter finding may mimic pancreatic intraductal papillary mucinous neoplasm [10, 22, 36]. On the opposite, direct extent of tumor into the pancreatic duct was not observed in PDA.

Our study has several limitations. First, the retrospective design has induced selection bias. A second limitation relates to the relatively small number of patients, but pancreatic ACC is a relatively rare tumor and most studies reporting imaging features of ACC are small series. A third limitation is that our comparative study was based on a 1:1 match so that a different match (*i.e.*, 1/2 or 1/3) might have yielded different results. A forth limitation is that we did not include a delayed phase of enhancement in our CT protocol to compare the enhancement patterns of pancreatic ACC to those of PDA on this specific phase. Finally, we have compared pancreatic ACC to PDA, although other pancreatic tumors may mimic ACC [32].

In conclusion, pancreatic ACC mostly presents as an enhancing, predominantly oval and purely solid pancreatic mass that is most frequently associated with visible lymph nodes, adjacent organ involvement and no bile duct dilatation by comparison with PDA. Knowledge of these discriminating findings may help clinicians and pathologists consider the diagnosis of ACC in patients with pancreatic tumors.

Authorship requirements

All the authors had fully participated to the study and approved the final draft.

Conflicts of interest

The authors have no conflicts of interest to disclose in relation with this study.

Funding

This research received no financial support.

References

1. Frampas E, David A, Regenet N, Touchefeu Y, Meyer J, Morla O. Pancreatic carcinoma: key-points from diagnosis to treatment. Diagn Interv Imaging 2016;97:1207-1223.
2. Barral M, Faraoun SA, Fishman EK, Dohan A, Pozzessere C, Berthelin MA, et al. Imaging features of rare pancreatic tumors. Diagn Interv Imaging 2016;97: 1259-1273.
3. Chu LC, Singhi AD, Haroun RR, Hruban RH, Fishman EK. The many faces of pancreatic serous cystadenoma: radiologic and pathologic correlation. Diagn Interv Imaging 2017;98: 191-202.
4. Bezerra ROF, Machado MC, Dos Santos Mota MM, Ezzedine TA, Siqueira LTB, Cerri GG. Rare pancreatic masses: a pictorial review of radiological concepts. Clin Imaging 2018;50: 314-323.
5. Jornet D, Soyer P, Terris B, Hoeffel C, Oudjit A, Legmann P, Gaujoux S, Barret M, Dohan A. MR imaging features of pancreatic acinar cell carcinoma. Diagn Interv Imaging 2019;100: 427-435.
6. Yeh R, Steinman J, Luk L, Kluger MD, Hecht EM. Imaging of pancreatic cancer: what the surgeon wants to know. Clin Imaging 2017; 42:203-217.
7. Holen KD, Klimstra DS, Hummer A, Gonen M, Conlon K, Brennan M, Saltz LB. Clinical characteristics and outcomes from an institutional series of acinar cell carcinoma of the pancreas and related tumors. J Clin Oncol 2002;20: 4673-4678.
8. Matos JM, Schmidt CM, Turrini O, Agaram NP, Niedergethmann M, Saeger HD, et al. Pancreatic acinar cell carcinoma: a multi-institutional study. J Gastrointest Surg 2009;13: 1495-1502
9. Matsumoto S, Sata N, Koizumi M, Lefor A, Yasuda Y. Imaging and pathological characteristics of small acinar cell carcinomas of the pancreas: a report of 3 cases. Pancreatology 2013;13: 320-323
10. Bhosale P, Balachandran A, Wang H, Wei W, Hwang RF, Fleming JB, et al. CT imaging features of acinar cell carcinoma and its hepatic metastases. Abdom Imaging 2013;38: 1383-1390.
11. Wang Y, Wang S, Zhou X, Zhou H, Cui Y, Li Q et al. Acinar cell carcinoma: a report of 19 cases with a brief review of the literature. World J Surg Oncol 2016;14: 172.

12. Shah S, Mortele KJ. Uncommon solid pancreatic neoplasms: ultrasound, computed tomography, and magnetic resonance imaging features. Semin Ultrasound CT MR 2007;28: 357-370.

13. Ong MJ, Tang YL, Tan CH. Clinics in diagnostic imaging (157). Acinar cell carcinoma (ACC) of the pancreatic tail. Singapore Med J 2014;55:564-567.

14. Liu K, Peng W, Zhou Z. The CT findings of pancreatic acinar cell carcinoma in five cases. Clin Imaging 2013;37: 302-307.

15. Chiou YY, Chiang JH, Hwang JI, Yen CH, Tsay SH, Chang CY. Acinar cell carcinoma of the pancreas: clinical and computed tomography manifestations. J Comput Assist Tomogr 2004;28: 180-186.

16. Raman SP, Hruban RH, Cameron JL, Wolfgang CL, Kawamoto S, Fishman EK. Acinar cell carcinoma of the pancreas: computed tomography features--a study of 15 patients. Abdom Imaging 2013;38: 137-143.

17. Mustert BR, Stafford-Johnson DB, Francis IR. Appearance of acinar cell carcinoma of the pancreas on dual-phase CT. AJR Am J Roentgenol 1998;171: 1709.

18. Hu S, Hu S, Wang M, Wu Z, Miao F. Clinical and CT imaging features of pancreatic acinar cell carcinoma. Radiol Med 2013;118: 723-731.

19. Yang TM, Han SC, Wu CJ, Mo LR. Acinar cell carcinomas with exophytic growth and intraductal pancreatic duct invasion: peculiar multislice computed tomographic picture. J Hepatobiliary Pancreat Surg 2009;16: 238-241.

20. Hashimoto M, Matsuda M, Watanabe G, Mori M, Motoi N, Nagai K, et al. Acinar cell carcinoma of the pancreas with intraductal growth: report of a case. Pancreas 2003;26: 306–308.

21. Luo Y, Hu G, Ma Y, Guo N, Li F. Acinar cell carcinoma of the pancreas presenting as diffuse pancreatic enlargement: two case reports and literature review. Medicine (Baltimore) 2017;96: e7904.

22. Sumiyoshi T, Shima Y, Okabayashi T, Kozuki A, Nakamura T. Comparison of pancreatic acinar cell carcinoma and adenocarcinoma using multidetector-row computed tomography. World J Gastroenterol 2013; 19: 5713-5719

23. Amin MB, editor. AJCC Cancer Staging Manual (8th ed). Pancreatic adenocarcinoma. New York, NY: Springer-Verlag; 2016.

24. Freeman GH, Halton JH. Note on exact treatment of contingency, goodness of fit and other problems of significance. Biometrika 1951;38: 141-149.

25. Tatli S, Mortele KJ, Levy AD, Glickman JN, Ros PR, Banks PA, et al. CT and MRI features of pure acinar cell carcinoma of the pancreas in adults. AJR Am J Roentgenol 2005;184: 511-519.

26. Hsu MY, Pan KT, Chu SY, Hung CF, Wu RC, Tseng JH. CT and MRI features of acinar cell carcinoma of the pancreas with pathological correlations. Clin Radiol 2010;65: 223-229.

27. Nagata S, Tomoeda M, Kubo C, Yoshizawa H, Yuki M, Kitamura M, et al. Intraductal polypoid growth variant of pancreatic acinar cell carcinoma metastasizing to the intrahepatic bile duct 6 years after surgery: a case report and literature review. Pancreatology 2012;12: 23-26.

28. Eriguchi N, Aoyagi S, Hara M, Okuda K, Saito N, Fukuda S, Akashi H, Kutami R, Jimi A. Large acinar cell carcinoma of the pancreas in a patient with elevated serum AFP level. J Hepatobiliary Pancreat Surg 2000;7: 222-5.

29. Sahani D, Prasad SR, Maher M, Warshaw AL, Hahn PF, Saini S. Functioning acinar cell pancreatic carcinoma: diagnosis on mangafodipir trisodium (Mn-DPDP)-enhanced MRI. J Comput Assist Tomogr 2002;26: 126-8.

30. Gravante G, Williams RN, Dennison AR, Bowrey DJ. Pancreatic acinar cell carcinoma. Surgery 2012;152: 138-139.

31. Khalili M, Wax BN, Reed WP, Schuss A, Drexler S, Weston SR, Katz DS. Radiology-pathology conference: acinar cell carcinoma of the pancreas. Clin Imaging 2006;30: 343-346.

32. Guerrache Y, Soyer P, Dohan A, Faraoun SA, Laurent V, Tasu JP, et al. Solid-pseudopapillary tumor of the pancreas: MR imaging findings in 21 patients. Clin Imaging 2014;38: 475-482.

33. Javadi S, Menias CO, Korivi BR, Shaaban AM, Patnana M, Alhalabi K, et al. Pancreatic calcifications and calcified pancreatic masses: pattern recognition approach on CT. AJR Am J Roentgenol 2017;209: 77-87.

34. Campisi A, Brancatelli G, Vullierme MP, Levy P, Ruszniewski P, Vilgrain V. Are pancreatic calcifications specific for the diagnosis of chronic pancreatitis? A multidetector-row CT analysis. Clin Radiol 2009;64: 903-911.

35. Mergo PJ, Helmberger TK, Buetow PC, Helmberger RC, Ros PR. Pancreatic neoplasms: MR imaging and pathologic correlation. Radiographics 1997;17: 281-301.

36. Kim HJ, Kim YK, Jang KT, Lim JH. Intraductal growing acinar cell carcinoma of the pancreas. Abdom Imaging 2013;38: 1115-1119.

Legends for figures

Figure 1. Flowchart of the selection of patients with acinar cell carcinoma of the pancreas.

Figure 2. Computed tomography examination (CT) examination in a 52-year-old man with acinar cell carcinoma of the pancreatic head. **A**, Plain CT image in the transverse plane shows homogeneous tumor (arrow) of the pancreatic head. No calcifications are present. **B**, CT image of the abdomen in the transverse plane obtained during the arterial phase of enhancement shows homogeneous, enhancing, purely solid tumor of the pancreatic head. Retroperitoneal, enlarged lymph nodes (arrowheads) are present. **C**, CT image of the abdomen in the transverse plane obtained during the portal venous phase of enhancement shows homogeneous, purely solid tumor of the pancreatic head. **D**, At a upper level, CT image of the abdomen in the transverse plane obtained during the portal venous phase of enhancement shows enlarged lymph node at the portacaval space (arrowhead). No intrahepatic bile duct dilatation is present.

Figure 3. Computed tomography examination (CT) examination in an 86-year-old man with acinar cell carcinoma of the pancreatic head. **A**, Plain CT image in the transverse plane shows large, exophytic tumor (arrow) of the pancreatic head. No calcifications are present. **B**, CT image of the abdomen in the transverse plane obtained during the arterial phase of enhancement shows slightly heterogenous, enhancing tumor of the pancreatic head. Duodenal involvement is present (arrowhead). **C**, CT image of the abdomen in the transverse plane obtained during the portal venous phase of enhancement shows tumor encapsulation (arrowhead).

Figure 4. Computed tomography examination (CT) examination in a 61-year-old woman with acinar cell carcinoma of the pancreatic body and tail. CT image of the abdomen in the transverse plane obtained during the portal venous phase of enhancement shows large pancreatic tumor invading the gastric wall (white arrow). Splenic vein encasement (white arrowhead) by tumor is responsible of segmental portal hypertension. Hepatic metastases (black arrowheads) and internal calcifications (black arrows) are present.

Table 1. Demographics of 20 patients with acinar cell cancer of the pancreas and 20 patients with pancreatic ductal adenocarcinoma.

Table 2. Classification of criteria used for image analysis on CT imaging in 20 patients with pancreatic acinar cell carcinoma and 20 patients with pancreatic adenocarcinoma.

Table 3. Comparison of CT imaging findings in 20 patients with pancreatic acinar cell carcinoma and 20 patients with pancreatic ductal adenocarcinoma.

Table 4. Estimated values of categorical variables for the diagnosis of acinar cell carcinoma of the pancreas in 40 patients.

Table 5. Results of univariate analysis with a conditional logistic regression model for 40 patients.

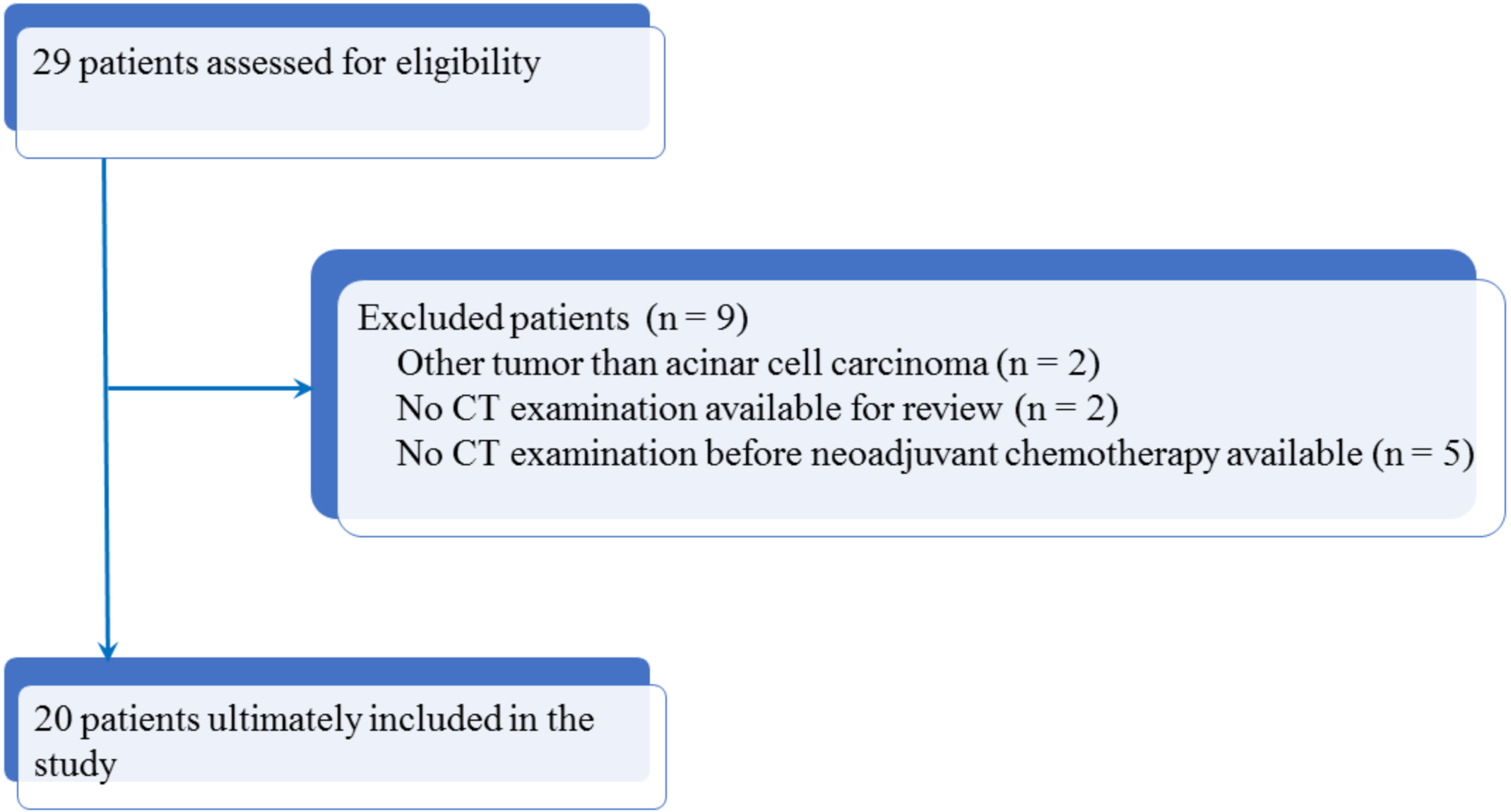
29 patients assessed for eligibility
Excluded patients (n = 9)
Other tumor than acinar cell carcinoma (n = 2)
No CT examination available for review (n = 2)
No CT examination before neoadjuvant chemotherapy available (n = 5)
20 patients ultimately included in the study

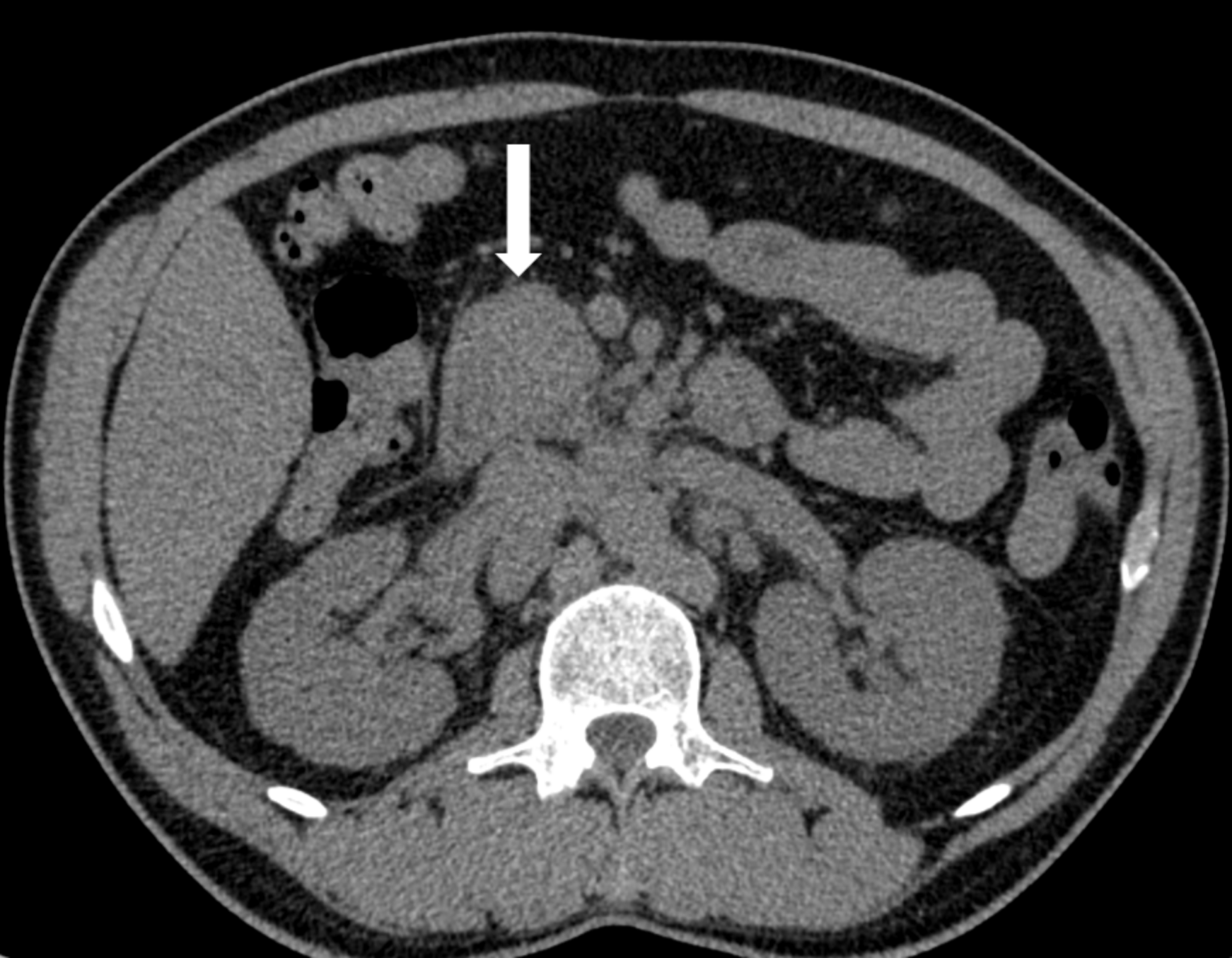

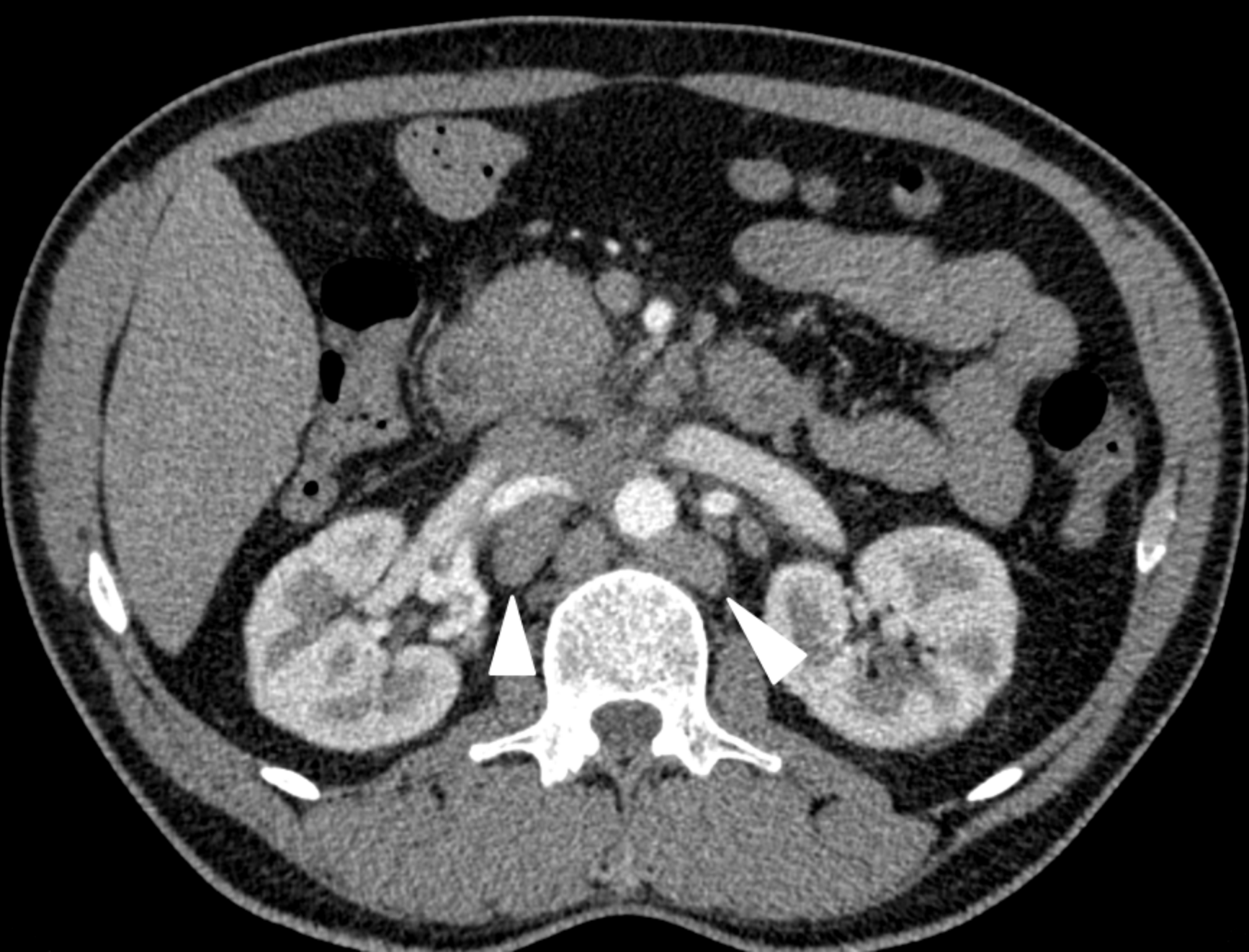

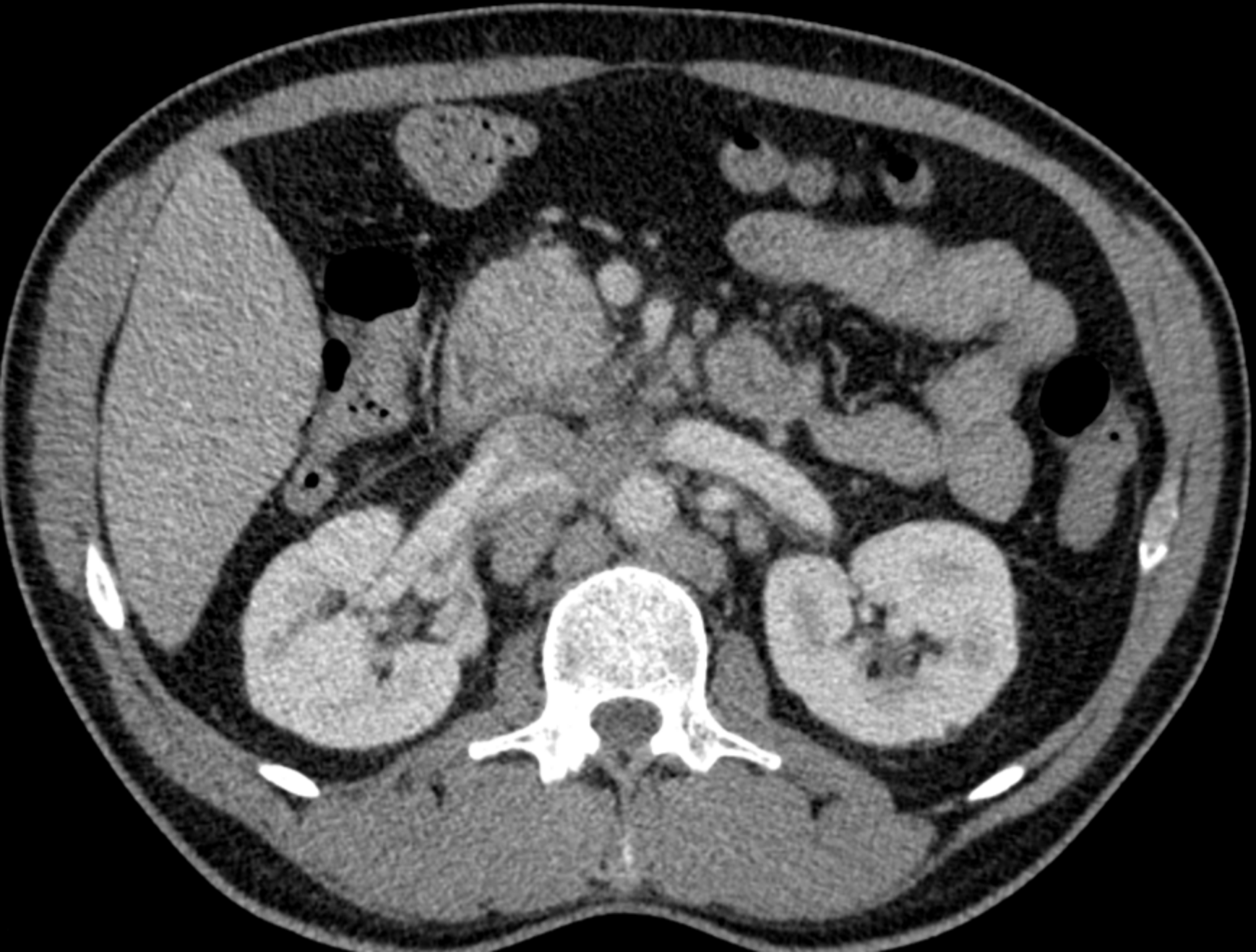

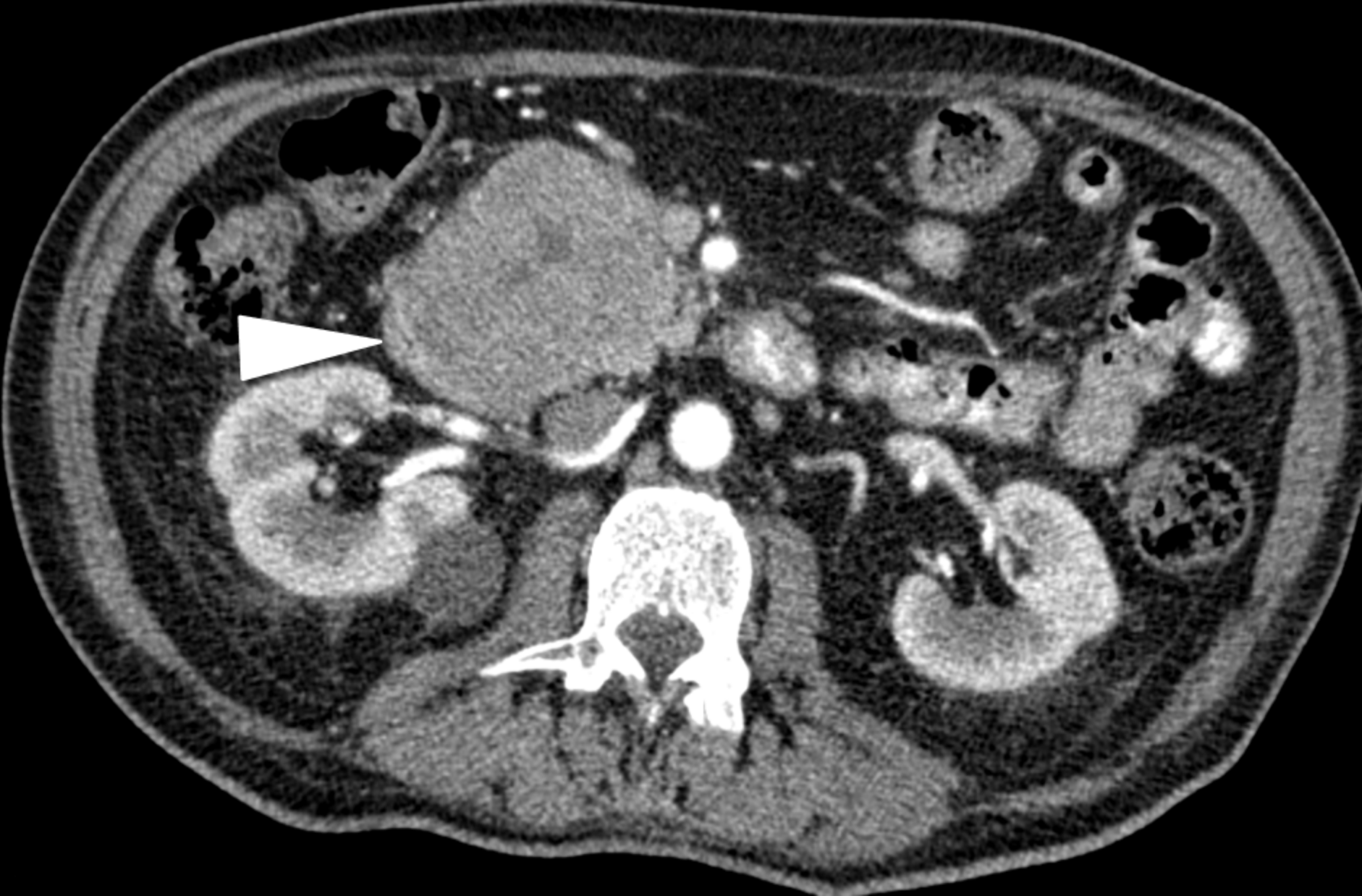

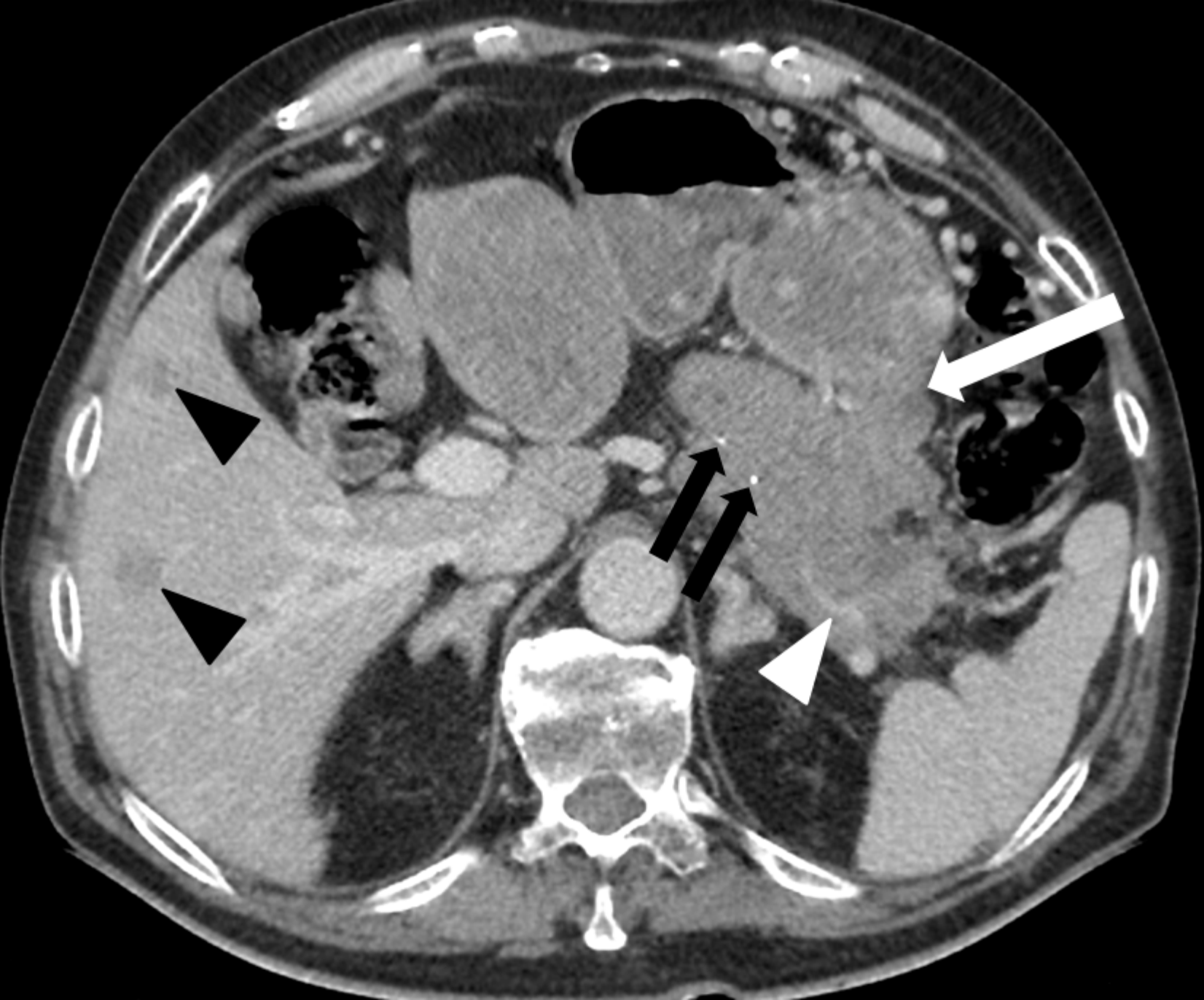

Variable	**All patients (n=40)**	**ACC group (n=20)**	**PDA group (n=20)**	***P value***
Mean age (years)				0.285*
Mean ± SD	64.2 ± 9.4	66.5 ± 10.7	61.8 ± 7.5	
(median; Q1, Q3)	(63; 57, 68.3)	(64.5; 59.8, 71)	(61; 57, 68)	
[range]	[43-88]	[51-88]	[43-74]	
Gender				> 0.999ǂ
Men	26 (26/40; 65 %)	13 (13/20; 65 %)	13 (13/20; 65 %)	
Women	14 (14/40; 35 %)	7 (7/20; 25 %)	7 (7/20; 25 %)	
Histopathological diagnosis				> 0.999ǂ
Percutaneous biopsy	18 (18/40; 45 %)	9 (9/20; 45 %)	9 (9/20; 45 %)	
Surgical biopsy	22 (22/40; 55 %)	11 (11/20; 55 %)	11 (11/20; 55 %)	
Primary tumor (T)				0.697†
T1	0 (0/40; 0%)	0 (0/20; 0 %)	0 (0/20; 0 %)	
T2	11 (11/40; 27 %)	6 (6/20; 30 %)	5 (5/20; 25 %)	
T3	14 (14/40; 35 %)	8 (8/20; 40 %)	6 (6/20; 30 %)	
T4	15 (15/40; 38 %)	6 (6/20; 30 %)	9 (9/20; 45 %)	
Regional lymph nodes (N)				0.806†
N0	16 (16/40; 40 %)	7 (7/20; 35 %)	9 (9/20; 45 %)	
N1	17 (17/40; 42 %)	9 (9/20; 45 %)	8 (8/20; 40 %)	
N2	7 (7/40; 18 %)	4 (4/20; 20 %)	3 (3/20; 15 %)	
Distant metastases (M)				0.333ǂ
M0	24 (24/40; 60 %)	10 (10/20; 50 %)	14 (14/20; 70 %)	
M1	16 (16/40; 40 %)	10 (10/20; 50 %)	6 (6/20; 30 %)	
Stage				0.149†
Stage IA	0 (0/40; 0 %)	0 (0/20; 0 %)	0 (0/20; 0 %)	
Stage IB	5 (5/40; 12 %)	2 (2/20; 10 %)	3 (3/20; 15 %)	
Stage IIA	6 (6/40; 15 %)	4 (4/20; 20 %)	2 (2/20; 10 %)	
Stage IIB	5 (5/40; 12 %)	0 (0/20; 0 %)	5 (5/20; 25 %)	
Stage 3	8 (8/40; 20 %)	4 (4/20; 20 %)	4 (4/20; 20 %)	
Stage 4	16 (16/40; 40 %)	10 (10/20; 50 %)	6 (6/20; 30 %)	
Surgical resection	22 (22/40; 55 %)	11 (11/20; 55 %)	11 (11/20; 55 %)	> 0.999ǂ

Note. ACC indicates acinar cell carcinoma. PDA indicates ductal adenocarcinoma. SD indicates standard deviation. Q1 indicates first quartile. Q3 indicates third quartile. Numbers in brackets are ranges. * Mann Whitney U test, ǂ Fisher exact test, † Freeman-Halton.

Quantitative criteria	**Categoric criteria**
Tumor largest diameter (mm)	Tumor location (head, body, tail)
Visible lymph node diameter (mm)	Tumor shape (round, oval)
	Tumor margins (well or ill-defined contours)
	Tumor capsule (yes, no)
	Tumor content (purely solid, cystic, mixed)
	Internal necrosis/hemorrhage (yes, no)
	Tumor enhancement (yes, no)
	Tumor homogeneneous enhancement (yes, no)
	Tumor enhancement on arterial phase* (>, =, <)
	Tumor enhancement on portal phase* (>, =, <)
	Tumor calcification (yes, no)
	Wirsung duct enlargement (yes, no)
	Upstream pancreatic atrophy
	Vascular involvement (yes, no)
	Segmental portal hypertension (yes, no)
	Hepatic metastases (yes, no)
	Bile duct dilatation (yes, no)
	Visible lymph nodes (yes, no)
	Direct adjacent organ involvement (yes, no)
	Ascites (yes, no)

Note. - Tumor enhancement was compared to enhancement of the apparently normal pancreatic gland parenchyma

Variable		Acinar cell carcinoma	Adenocarcinoma	*P* value
Quantitative variables				
Largest tumor diameter (mm)		52.6 ± 28.0 [24 – 120] (43.5; 33.3, 54)	36.8 ± 8.3 [24-59] (37.5; 30.5, 40.5)	0.058*
Visible lymph node size (mm)		14 ± 4.8 [7-25] (14; 11.5, 14.5)	8.8 ± 4.1 [5-15] (8; 6.3, 11.3)	**0.039***
Qualitative variables				
Tumor location				0.675ǂ
	Head	9 (9/20; 45 %)	9 (9/20; 45 %)	
	Body	6 (6/20; 30 %)	8 (8/20; 40 %)	
	Tail	5 (5/20; 25 %)	3 (3/20; 15 %)	
Tumor shape				0.407ǂ
	Oval	15 (15/20; 75 %)	18 (18/20; 90 %)	
	Round	5 (5/20; 25 %)	2 (2/20; 10 %)	
Well defined tumor margins		14 (14/20; 70 %)	5 (5/20; 25 %)	**0.005**
Tumor capsule		3 (3/20; 15 %)	0 (0/20; 0 %)	0.231ǂ
Purely solid content		13 (13/20; 65 %)	12 (12/20; 60 %)	> 0.999ǂ
Internal necrosis/hemorrhage		7 (7/20; 35 %)	8 (8/20; 40 %)	> 0.999ǂ
Tumor enhancement		20 (20/20; 100 %)	20 (20/20; 100 %)	> 0.999ǂ
Homogeneous tumor enhancement		11 (11/20; 55 %)	8 (8/20; 40%)	0.264
Hypoattenuating tumor on arterial phase		9 (9/20; 45 %)	17 (17/20; 85 %)	**0.009**
Hypoattenuating tumor on portal phase		8 (8/20; 40 %)	13 (13/20; 65 %)	0.102
Tumor calcification		2 (2/20; 10 %)	0 (0/20; 0 %)	0.244ǂ
Wirsung duct > 4 mm		6 (6/20; 30 %)	10 (10/20; 50 %)	0.333ǂ
Upstream pancreatic atrophy		8 (8/20; 40 %)	8 (8/20; 40 %)	0.626
Vascular involvement		9 (9/20; 45 %)	14 (14/20; 70 %)	0.200ǂ
Segmental portal hypertension		5 (5/20; 25 %)	5 (5/20; 25 %)	>0.999ǂ
Hepatic metastases		10 (10/20; 50 %)	6 (6/20; 30 %)	0.333ǂ
No bile duct dilatation		2 (2/20; 10 %)	10 (10/20; 50 %)	**0.014**ǂ
Visible lymph nodes		14 (14/20; 70 %)	7 (7/20; 35 %)	0.056ǂ
Adjacent organ involvement		10 (10/20; 50 %)	3 (3/20; 15 %)	**0.041**ǂ
Ascites		3 (3/20; 15 %)	3 (3/20; 15 %)	> 0.999ǂ

Note. Qualitative variables are expressed as raw numbers; numbers in parentheses are proportions, followed by percentages. Quantitative variables are expressed as mean ±

standard deviation (SD); numbers in brackets are ranges; numbers in parentheses are median followed by first (Q1) and third (Q3) quartiles. Bold indicates significant differences.
* Mann Whitney U test; ǂ Fisher exact test

Variable	TP	FP	FN	TN	Sensitivity (%)	Specificity (%)	Accuracy (%)
Tumor shape (round)	5	2	15	18	25 (5/20) [9-49]	90 (18/20) [68-99]	58 (23/40 [41-73]
Well defined tumor margins	14	5	6	15	70 (14/20) [46-88]	75 (15/20) [51-91]	73 (29/40) [56-85]
Tumor capsule	3	0	17	20	15 (3/20) [3-38]	100 (20/20) [83-100]	58 (23/40) [41-73]
Purely solid content	13	12	7	8	65 (13/20) [41-85]	40 (8/20) [19-64]	53 (21/40) [36-68]
No internal necrosis/hemorrhage	13	12	7	8	65 (13/20) [41-85]	40 (8/20) [19-64]	53 (21/40) [36-68]
Tumor enhancement	20	20	0	0	100 (20/20) [83-100]	0 (0/20) [0-17]	50 (20/40) [34-66]
Homogeneous enhancement	11	8	9	12	55 (11/20) [32-77]	60 (12/20) [36-81]	58 (23/40) [41-73]
Hypoattenuating tumor on arterial phase	9	17	11	3	45 (9/20) [23-68]	15 (3/20) [3-38]	30 (12/40) [17-47]
Hypoattenuating tumor on portal phase	8	13	12	7	40 (8/20) [19-64]	35 (7/20) [15-59]	28 (15/40) [23-54]
Tumor calcification	2	0	18	20	10 (2/20) [1-32]	100 (20/20) [83-100]	55 (22/40) [38-71]
Wirsung duct ≤ 4 mm	14	10	6	10	70 (14/20) [46-88]	50 (10/20) [27-73]	60 (24/40) [43-75]
Upstream pancreatic atrophy	8	8	12	12	40 (8/20) [19-64]	60 (12/20) [36-81]	50 (20/40) [34-66]
No vascular involvement	11	6	9	14	55 (11/20) [32-77]	70 (14/20) [46-88]	63 (25/40) [46-77]
Segmental portal hypertension	5	5	15	15	25 (5/20) [9-49]	75 (15/20) [51-91]	50 (20/40) [34-66]
Hepatic metastases	10	4	10	16	50 (10/20) [27-73]	85 (16/20) [62-97]	65 (26/40) [48-79]
No bile duct dilatation	18	10	2	10	90 (18/20) [68-99]	50 (10/20) [27-73]	70 (28/40) [53-83]
Visible lymph nodes	14	7	6	13	70 (14/20) [46-88]	65 (13/20) [41-85]	68 (27/40) [51-81]
Adjacent organ involvement	10	3	10	17	50 (10/20) [27-73]	85 (17/20) [62-97]	68 (27/40) [51-81]
Ascites	3	3	17	17	15 (3/20) [3-38]	85 (17/20) [62-97]	50 (20/40) [34-66]

Note. TP = true positive. FP = false positive. FN = false negative. TN = true negative. Se = sensitivity (TP/TP+FN). Sp = specificity (TN/TN+FP). Ac = accuracy (TP+TN/TP+FP+TN+FN). Numbers in parentheses are proportions used to calculate the percentages. Numbers in brackets are exact 95% confidence intervals. All percentages were rounded with no decimals.

Effect*	**Results OR [95 %CI]**	***P* value**
Round shape	0.33 [0.06-1.97]	0.204
Tumor capsule	15 (3/20) *vs.* 0 (0/20) †	0.231‡
Well defined tumor margins	7.00 [1.74-18.17]	**0.005**
Purely solid content	1.24 [0.34-4.46]	0.500
Internal necrosis/hemorrhage	0.81 [0.22-2.91]	0.500
Tumor enhancement	20 (20/20) vs. 20 (20/20) †	>0.99‡
Homogeneous tumor enhancement	1.83 [0.52-6.43]	0.264
Hypoattenuating tumor on arterial phase	0.14 [0.03-0.65]	**0.010**
Hypoattenuating tumor on portal phase	0.36 [0.10-1.29]	0.100
Tumor calcification	10 (2/20) *vs.* 0 (0/20) †	0.244‡
Wirsung duct enlargement	0.43 [0.12-1.57]	0.167
Upstream pancreatic atrophy	1.00 [0;28-3.54]	0.63
Vascular involvement	0.35 [0.10-1.29]	0.100
Segmental portal hypertension	1.00 [0.24-4.18]	0.642‡
Hepatic metastases	0.43 [0.12-1.57]	0.167
No bile duct dilatation	9.00 [1.64-49.45]	**0.007**
Visible lymph nodes	4.33 [1.15-16.32]	**0.028**
Adjacent organ involvement	5.67 [1.25-25.61]	**0.020**
Ascites	1.00 [0.18-5.67]	0.669

Note. Unless otherwise noted, data are odds ratios, 95 % confidence intervals are in brackets. Odds ratio and 95 % CIs are not shown for some variable because a zero value for corresponding data in Table 3 led to unstable estimates of these parameters.

* All effects are present versus absent. Wirsung duct enlargement corresponds to a Wirsung duct diameter > 4 mm.

† Frequency of corresponding variable; data are percentages; proportions are in parentheses.

‡ Exact conditional logistic regression.

Computed tomography features of acinar cell carcinoma of the pancreas

Short title:

CT of acinar cell carcinoma

Maxime BARAT [a, b*], Anthony DOHAN [a, b], Sébastien GAUJOUX [b, c], Christine HOEFFEL [d], Diane JORNET [a], Ammar OUDJIT [a], Romain CORIAT [b, e], Maximilien BARRET [b, e], Benoît TERRIS [b,f], Philippe SOYER [a,b]

[a] Department of Radiology, Hôpital Cochin, AP-HP, 75014 Paris, France

[b] Université de Paris, Descartes-Paris 5, 75006 Paris, France

[c] Department of Abdominal Surgery, Hôpital Cochin, AP-HP, 75014 Paris, France

[d] Department of Radiology, Hôpital Robert Debré, 51092 Reims, France

[e] Department of Gastroenterology, Hôpital Cochin, AP-HP, 75014 Paris, France

[f] Department of Pathology, Hôpital Cochin, AP-HP, 75014 Paris, France

Corresponding author: maxime.barat@aphp.fr

Department of Radiology, Hôpital Cochin, AP-HP, 27 Rue du Faubourg Saint-Jacques, 75014 Paris, France